16 Method Used and Highlight Results Achieved in FLOMANIA

U. Bunge, C. Mockett, and F. Thiele, Technical University of Berlin (TUB)

Abstract

This chapter describes the method used by the Technical University of Berlin and it summarises the highlight results obtained with this method in the course of FLOMANIA. The main results are the successful implementation and calibration of DES for three different models and the improved representation of flow physics with these DES implementations.

16.1 Method used by TUB

16.1.1 Numerical method

The flow for all cases is computed numerically using an in-house finite-volume based code solving either the unsteady Reynolds-averaged or spatially filtered Navier-Stokes equations in case of a RANS or Large-Eddy simulation (LES), respectively. The procedure is implicit and of second order accuracy in space and time. All scalar quantities as well as the Cartesian components of tensorial quantities are stored in the cell centers of arbitrarily curvilinear, semi-structured grids. Diffusive terms are approximated with central schemes, whereas convective terms can be treated with central or upwind-biased limited schemes of higher order (Xue, 1998). A hybrid blending of both approaches for a Detached-Eddy Simulation (DES), as suggested by Travin et al., 2002 and discussed in chapter III-2 has been implemented, addressing the conflicting requirements posed by RANS and LES on the convection scheme. The linearized equations are solved sequentially and the pressure is iterated to convergence using a pressure-correction scheme of the SIMPLE type that assures mass conservation as the pressure equation is derived from the continuity equation (Karki and Patankar, 1989). Introducing apparent pressures and viscosities, a generalized Rhie & Chow interpolation is used to avoid an odd-even decoupling of pressure, velocity and Reynolds-stress components (Obi et al., 1991).

16.1.2 Turbulence Treatment

Turbulence is handled using three RANS turbulence models of different degrees of complexity, the details of which can be found in chapter III-2. The simplest is a modification of the SA model, the Strain-Adaptive Linear Spalart-Allmaras model (SALSA, Rung et al., 2003). Secondly, the linear local realizable (LLR) k-ω Model (Rung and Thiele, 1996), is a local linear two-parameter model derived from realizability and non-equilibrium turbulence constraints. Finally, the compact explicit algebraic stress model (CEASM, Lübcke et al., 2002), using the LL k-ε model as a background model (Lien and Leschziner, 1993) employs expressions

for the Reynolds stresses chosen to yield physically correct results for highly 3D flows whilst preserving the simplicity of the quadratic formulation.

As long as grids are fine enough, a hybrid boundary condition (Rung et al., 2000) assures a low-Re formulation or solution down to the wall for all models.

All three models are also used for DES, where the constant C_{DES} is calibrated by computing the decay of isotropic turbulence as described by Bunge et al., 2003, and in the following section. To achieve a DES, the turbulence length scale in the model is replaced by the DES grid length scale, and the precise manner in which this is achieved for each of the TUB turbulence models is given in the DES section of chapter III-2. It is interesting to note that of the two length scales present in the background model of the CEASM, the wall-normal distance is left unchanged, allowing the construction of a shielding function to avoid grid-induced separation.

16.2 Highlight Results

16.2.1 Calibration of C_{DES}

As the DES modification (see chapter III-2) causes the underlying turbulence model to act as a subgrid-scale model in the LES zones, a test case to validate this LES capability is required. Furthermore, as the DES modification introduces a new model parameter C_{DES}, a reliable method must be found to determine a calibrated value for this. Both of these issues can be addressed simultaneously, employing the case of decaying isotropic (homogenous) turbulence (DIT, Comte-Bellot and Corrsin, 1971), as described by Shur et al., 1999. Furthermore, this procedure is to be followed for each of the DES implementations based on the three turbulence models mentioned above.

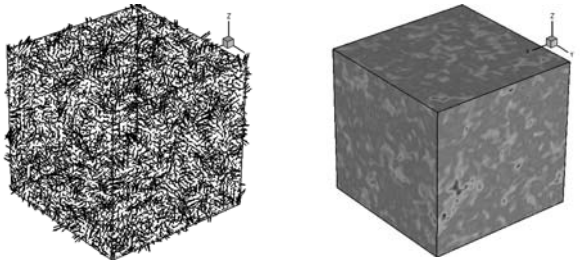

Figure 1 Initial velocity field and viscosity ratio for DIT

The decay of isotropic turbulence is simulated using three equidistant box grids of 16^3, 32^3 and 64^3 volumes, with periodic boundary conditions in all three directions. The flow field is initialised with a prescribed velocity field with zero mean flow, Fig. 1. This velocity distribution is obtained from the experimental energy distribution for t=0 using an inverse Fourier transformation from a tool provided by Prof. Strelets of SPTU. The same tool provides a means to extract an energy distribution from the computed velocity fields for comparison with experimental data at later time steps, as seen in Figs. 2 and 3.

Once an initial calibration investigation is complete, a deeper examination of the sensitivity of C_{DES} to variations of the underlying numerics is conducted.

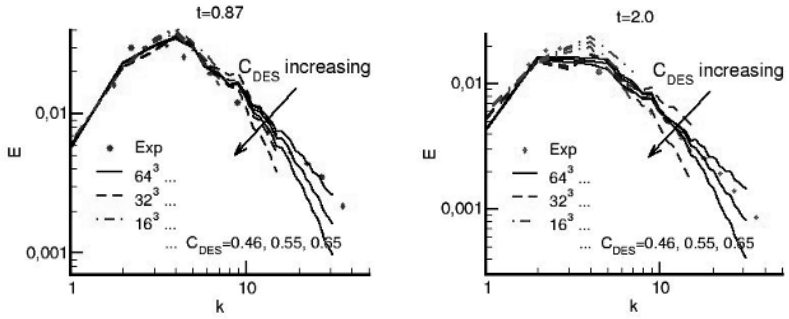

Figure 2 Calibration spectra for the SALSA model at t=0.87 (left) and t=2.0 (right)

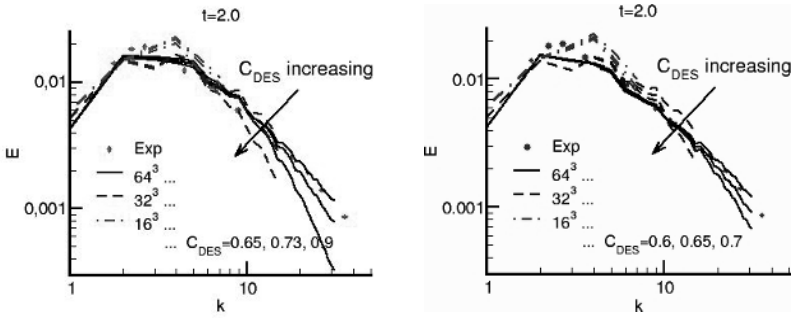

Figure 3 Calibration spectra for the LLR k-ω model (left) and the CEASM (right), at t=2.0

In Figs. 2 and 3, the resulting calibration spectra for each turbulence model are shown. The t=0.87 time point is shown only for one model (SALSA) as the long-term behaviour is more important. The results from the 32^3 grid were given precedence, as this was taken to be representative of the coarseness for practical applications. The level of dissipation in the underlying numerics can be varied using different flux blending parameters between upwind and central difference-based schemes. The effect of raising the dissipation is balanced by lower resulting C_{DES} values, Table 1, and is representative of realistic practical DES applications on coarser and less uniform grids.

Table 1 Range of applicable C_{DES} values for each model

Model:	Low dissipative:	Higher dissipative:
SALSA	0.65	0.55
LLR k-ω	0.78	0.73
CEASM	0.70	0.60

16.2.2 NACA0012 at high angle of attack

An application test case demonstrating the benefits of DES over URANS on the same grid is the computation of an airfoil in deep stall. In FLOMANIA, the NACA0012 profile was chosen at a range of angles of attack with Re=10^5, the complete set of results and a description of the grids for which can be found in chapter IV-6. Table 2 gives an overview for an angle of 60° of the mean lift (C_L) and drag (C_D) as well as the shedding frequency (St) for the coarse (c), medium (m) and fine (f) grids. The improvement of results in comparison to experimental data is evident.

Table 2 DES and URANS results on all the grids for 60° angle of attack in comparison to experiments for all models. Experimental force coefficient data as used by Strelets, 2001, Strouhal number from experiments of Swalwell et al., 2003

Model		CEASM			LLR k–ω			SALSA		
		$\overline{C}_L$	$\overline{C}_D$	St	$\overline{C}_L$	$\overline{C}_D$	St	$\overline{C}_L$	$\overline{C}_D$	St
Experiments		0.92	1.65	0.20	0.92	1.65	0.20	0.92	1.65	0.20
URANS	c	1.11	1.92	0.13	1.27	2.16	0.14	1.21	2.11	0.13
	m	1.08	1.83	0.13	1.19	1.99	0.16	1.12	1.93	0.12
	f	1.09	1.86	0.13	1.18	1.98	0.16	1.11	1.91	0.15
DES	c	0.97	1.63	0.17	0.93	1.57	0.18	0.91	1.53	0.17
	m	0.98	1.64	0.17	0.94	1.58	0.18	0.97	1.64	0.16
	f	0.92	1.56	0.18	0.94	1.58	0.20	0.95	1.59	0.18

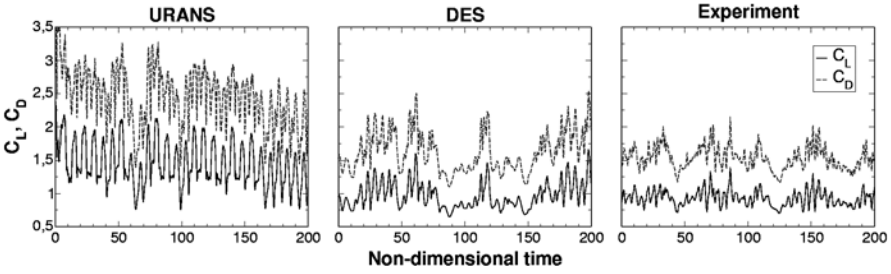

Figure 4 Lift vs. time for URANS, DES (CEASM) and experiments

Fig. 4 reveals that not only the frequency and mean value of lift and drag agree well with experimental data, but also the qualitative temporal behaviour is represented much better. The DES gives a more stochastic result with areas of reduced activity or "weak shedding cycles", which are also observed in the experiments and indicate a modulation between an organised flow pattern to a more chaotic one consisting of much finer structures.